blood®
Regular Article

HEMATOPOIESIS AND STEM CELLS

The neurotransmitter receptor Gabbr1 regulates proliferation and function of hematopoietic stem and progenitor cells

Lijian Shao,[1,2,*] Adedamola Elujoba-Bridenstine,[1,3,*] Katherine E. Zink,[4] Laura M. Sanchez,[4] Brian J. Cox,[5,6] Karen E. Pollok,[7-9] Anthony L. Sinn,[9] Barbara J. Bailey,[9] Emily C. Sims,[9] Scott H. Cooper,[10] Hal E. Broxmeyer,[9,10] Kostandin V. Pajcini,[1,†] and Owen J. Tamplin[1,3,†]

[1]Department of Pharmacology, University of Illinois at Chicago, Chicago, IL; [2]Department of Occupational Health and Toxicology, School of Public Health, Nanchang University, Nanchang, People's Republic of China; [3]Department of Cell and Regenerative Biology, University of Wisconsin-Madison, Madison, WI; [4]Department of Pharmaceutical Sciences, University of Illinois at Chicago, Chicago, IL; [5]Department of Physiology and [6]Department of Obstetrics and Gynaecology, University of Toronto, Toronto, ON, Canada; and [7]Department of Pharmacology and Toxicology, [8]Department of Pediatrics, [9]Melvin and Bren Simon Cancer Center, and [10]Department of Microbiology and Immunology, School of Medicine, Indiana University, Indianapolis, IN

KEY POINTS

- **Gabbr1 is involved in HSPC proliferation and B-cell differentiation.**
- **Treatment of human UCB progenitors with GABBR1 agonist results in increased long-term engraftment after transplantation.**

Hematopoietic and nervous systems are linked via innervation of bone marrow (BM) niche cells. Hematopoietic stem/progenitor cells (HSPCs) express neurotransmitter receptors, such as the γ-aminobutyric acid (GABA) type B receptor subunit 1 (GABBR1), suggesting that HSPCs could be directly regulated by neurotransmitters like GABA that directly bind to GABBR1. We performed imaging mass spectrometry and found that the endogenous GABA molecule is regionally localized and concentrated near the endosteum of the BM niche. To better understand the role of GABBR1 in regulating HSPCs, we generated a constitutive *Gabbr1*-knockout mouse model. Analysis revealed that HSPC numbers were significantly reduced in the BM compared with wild-type littermates. Moreover, *Gabbr1*-null hematopoietic stem cells had diminished capacity to reconstitute irradiated recipients in a competitive transplantation model. *Gabbr1*-null HSPCs were less proliferative under steady-state conditions and upon stress. Colony-forming unit assays demonstrated that almost all *Gabbr1*-null HSPCs were in a slow or noncycling state. In vitro differentiation of *Gabbr1*-null HSPCs in cocultures produced fewer overall cell numbers with significant defects in differentiation and expansion of the B-cell lineage. To determine whether a GABBR1 agonist could stimulate human umbilical cord blood (UCB) HSPCs, we performed brief ex vivo treatment prior to transplant into immunodeficient mice, with significant increases in long-term engraftment of HSPCs compared with GABBR1 antagonist or vehicle treatments. Our results indicate a direct role for GABBR1 in HSPC proliferation, and identify a potential target to improve HSPC engraftment in clinical transplantation. (*Blood*. 2021;137(6):775-787)

Introduction

Hematopoietic stem/progenitor cells (HSPCs) maintain hematopoiesis throughout life by self-renewal or multilineage differentiation to produce mature progeny.[1] The bone marrow (BM) serves as the HSPC microenvironment niche, where HSPCs receive signals regulating their proliferation, differentiation, or quiescence.[2] The nervous system innervates the BM niche, and regulates HSPCs during homeostasis and tissue regeneration.[3] The nervous system indirectly regulates HSPCs by modulating BM niche stromal cells.[4] However, there is also evidence for expression of neuroreceptors on HSPCs.[5-10]

γ-Aminobutyric acid (GABA) is the main inhibitory neurotransmitter in the central nervous system. It binds GABA A ligand-gated ion channel receptors, or GABA B G protein–coupled receptors.[11] GABA is also found in peripheral tissues such as pancreas, spleen, and lung.[12,13] Surprisingly, human CD34$^+$ and CD133$^+$ HSPCs express GABA type B receptor subunit 1 (GABBR1),[5,14] however, its function in hematopoiesis remains unknown. Using a CRISPR-generated global *Gabbr1*-knockout mouse model, we demonstrate that Gabbr1 can regulate the HSPC pool. *Gabbr1*-null mice showed decreased HSPC BM numbers and peripheral lymphoid cell numbers. Colony-forming unit (CFU) assays indicated that *Gabbr1*-null mice had few cycling progenitors. Significantly, *Gabbr1*-null HSPCs showed reduced proliferative ability and hematopoietic reconstitution. Expression profiling from *Gabbr1*-null HSPCs revealed significant deregulation of B-cell differentiation. Additionally, human CD34$^+$ umbilical cord blood (UCB) HSPCs treated with the GABBR1 agonist, baclofen, produced sustained increases in BM

chimerism and progenitor numbers for up to 16 weeks in a xenograft mouse model. This indicates that neuroreceptor GABBR1 is a critical regulator of the HSPC pool.

Materials and methods

Mouse strains

All mice were housed at University of Illinois Chicago (UIC) AAALAC-certified animal facilities. Food and water ad libitum were routinely given. The Institutional Animal Care and Use Committees of UIC approved all experimental procedures. C57/BL6 (CD45.2), CD45B6.SJL-*Ptprc*^{a}*Pep3*^{b}/BoyJ (CD45.1), and *Rag1*$^{-/-}$ mice[15] were purchased from The Jackson Laboratory (Bar Harbor, ME) or Charles River (Wilmington, MA). CD45.1/2 were generated by crossing CD45.1 females with CD45.2 males. *Gabbr1* C57/BL6–knockout (*Gabbr1*$^{-/-}$) mice were generated at the University of Chicago by CRISPR/Cas9 base pair insertion leading to a nonsense mutation. Postnatal day 13 and 15 (P13 and P15) *Gabbr1*$^{-/-}$ mice were used due to survival defects at P20.[16-18]

Imaging mass spectrometry

Femurs were harvested from female 6- to 8-week-old C57/BL6 mice, frozen fresh in 2% carboxymethylcellulose (217277; EMD Millipore) in prechilled hexane on dry ice, and stored at −80°C. Bones were sectioned at 10 μm using MX35 blades (Thermo Scientific) on a Leica CM 1850 UV cryostat. We adhered the copper tape to the slides prior to collection and a roll plate was necessary to keep samples from fracturing. After femurs were adhered to indium tin-oxide–coated glass sides (Bruker Daltonics) using double-sided copper conductive tape (Electron Microscopy Sciences), samples were prepared for matrix-assisted laser desorption/ionization time-of-flight imaging mass spectrometry (IMS).

Analysis of hematopoietic populations

After isolation and cellularization of BM and fetal liver (FL) hematopoietic cells, antibody staining was performed, followed by flow cytometry (BD LSRFortessa Flow Cytometer; BD Biosciences). Details of antibodies are in supplemental Table 1 (available on the *Blood* Web site). Data were analyzed using FACSDiva 6.0 (BD Biosciences) and FlowJo software.

Noncompetitive stem cell transplantation

BM cells (1×10^6) harvested from 3 pooled P15 *Gabbr1*$^{+/+}$ or *Gabbr1*$^{-/-}$ littermate mice were transplanted into lethally irradiated CD45.1 recipients. For hematopoietic stem cell (HSC) transplantation, 350 HSCs (Lin$^-$/Sca1$^+$/cKit$^+$/CD48$^-$/CD150$^+$) from BM of *Gabbr1*$^{+/+}$ or *Gabbr1*$^{-/-}$ mice were injected into irradiated CD45.1 recipients with 5×10^5 CD45.1/2 spleen cells. Recipients were maintained on antibiotic water for 1 week before, and 2 weeks after, transplantation. Donor reconstitution was measured in peripheral blood (PB; at 1, 2, 3 months, lysed with ACK lysis buffer), and BM at 3 months. Details of antibodies are in supplemental Table 1.

Competitive transplantation

For primary competitive transplantation, 350 HSCs (Lin$^-$/Sca1$^+$/cKit$^+$/CD48$^-$/CD150$^+$) from 3 to 4 *Gabbr1*$^{+/+}$ or *Gabbr1*$^{-/-}$ littermates (CD45.2) were sorted and mixed with 350 competitor HSCs pooled from 3 to 4 CD45.1/2 wild-type (WT) mice. Mixed cells were retro-orbitally transplanted into lethally irradiated congenic CD45.1 recipients with 5×10^5 CD45.1 spleen cells. Donor reconstitution was evaluated as above (see "Noncompetitive stem cell transplantation"). Secondary transplants followed (see supplemental Methods).

Supplemental methods

Further details on sample processing, other assays, and bioinformatic analyses are in supplemental Methods.

Results

HSPCs express Gabbr1

We investigated receptor *Gabbr1* expression in mouse HSPCs and presence of its neurotransmitter, GABA, in the BM. Published HSPC microarray and single-cell RNA-sequencing (RNA-seq) data were reanalyzed for *Gabbr1* expression. A recent study[19] did not score *Gabbr1* as expressed in HSPCs because of low levels in bulk microarray data from Gene Expression Commons (GEXC).[20] Despite low expression levels of *Gabbr1* in HSPCs, relative levels are higher in HSCs compared with more differentiated progenitors, with the exception of common lymphoid progenitors (CLPs) that have the highest expression level of *Gabbr1* (Figure 1A; supplemental Figure 1A).[21] We analyzed single-cell RNA-seq data from 3 independent studies that detected *Gabbr1* in a subset of HSPCs (Figure 1B, and data not shown).[22-24] In order to confirm published results, we used flow cytometry to test for Gabbr1 receptor surface expression in BM HSPCs. A distinct population of Lin$^-$Sca1$^+$cKit$^+$ (LSK) progenitors (~12%) and HSCs (LSK/CD48$^-$/CD150$^+$; ~15%) has detectable Gabbr1 surface expression (Figure 1C), indicating that *Gabbr1* is expressed in a subset of BM-resident HSPCs, including HSCs.

GABA is present in the adult BM endosteal region

We set out to identify the cell type that produces GABA in BM, based on expression of glutamate decarboxylase enzymes GAD1 or GAD2 that convert glutamic acid to GABA.[25] It was suggested that non-neural cells in the BM were candidates for GABA production, however, the specific cell type was not determined.[19] Single-cell RNA-seq data of BM stromal cells did not reveal a cell type clearly expressing *Gad1* or *Gad2*.[26] However, Haemopedia RNA-seq and microarray data of mouse hematopoietic populations found that *Gad1* (but not *Gad2*) was strongly enriched in B cells (supplemental Figure 1B).[27,28] Quantitative reverse transcription polymerase chain reaction (RT-qPCR) analysis of sorted B cells confirmed expression of *Gad1* transcript (Figure 1D). Intracellular flow cytometry analysis of B220$^+$CD93$^-$ B cells found that 77.7% were positive for Gad1, whereas CD11b$^+$ myeloid cells were negative (Figure 1E). These results were confirmed by immunofluorescence analysis of mouse BM sternum that showed B220$^+$ B cells, but not CD11b$^+$ myeloid cells, were positive for Gad1 (Figure 1F). We repeated intracellular flow cytometry and immunofluorescence analysis using BM from *Rag1*$^{-/-}$ mutants that lack B cells.[15] Gad1 expression was largely absent in BM of these B-cell–deficient mutants (supplemental Figure 1C-D). Together, this establishes Gabbr1 receptor expression by a subset of HSPCs, including HSCs, and that B cells express Gad1 enzyme.

We determined whether endogenous GABA molecules are present in the BM. To achieve spatial mapping of GABA across different regions of the BM niche, we performed IMS analysis.[29]

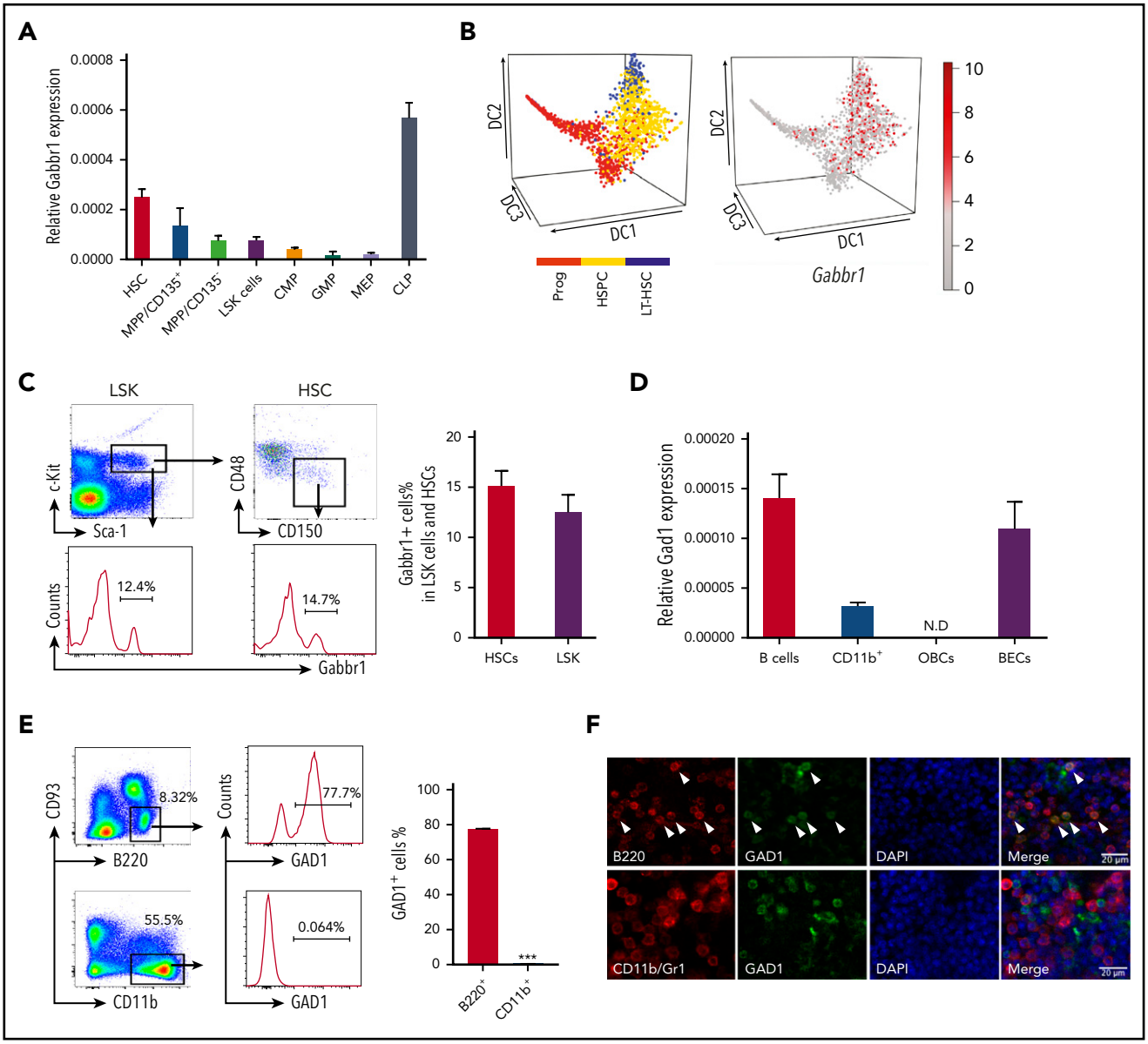

Figure 1. HSPCs express GABA B receptor Gabbr1 and B-cell lineages express glutamate decarboxylase Gad1. (A) RT-qPCR of relative *Gabbr1* expression in sorted HSPC populations. (B) Published single-cell RNA-seq data detected *Gabbr1* in a subset of HSPCs.[22] (C) Representative flow cytometry data and bar graph showing ~12% of Lin$^-$ Sca1$^+$cKit$^+$ (LSK) progenitors, and ~15% of HSCs (LSK/CD48$^-$/CD150$^+$) express cell-surface Gabbr1 receptor. (D) RT-qPCR analysis of *Gad1* expression in sorted phenotypic B cells (B220$^+$), CD11b$^+$ cells, osteoblastic cells (OBCs), and BM endothelial cells (BECs) (n = 3, from 2 independent experiments). (E) Representative intracellular flow cytometry data and bar graph showing that 77.7% of B220$^+$/CD93$^-$ cells express Gad1, compared with CD11b$^+$ cells that express almost none (n = 3, from 2 independent experiments). ***$P < .001$. (F) Immunofluorescent antibody staining (scale bar, 20 µm) of sternum BM showing that Gad1 (green) is expressed in B220$^+$ (red) B cells (arrowheads point to cells that express both markers). Gad1 is not expressed in Cd11b$^+$/Gr1$^+$ myeloid cells (representative of n = 9 sternum regions from n = 4 mice) (see also supplemental Figure 1). CMP, common myeloid progenitor; DAPI, 4′,6-diamidino-2-phenylindole; GMP, granulocyte-macrophage progenitor; LT-HSC, long-term HSC; MEP, megakaryocyte-erythroid progenitor; MPP, multipotent progenitor; N.D., not determined; Prog, progenitor.

IMS is label-free and allows for direct detection and relative quantification of endogenous metabolites. Femur sections from WT adult mice were spotted with commercial GABA standard as an internal control (supplemental Figure 2A-B). IMS was performed at a spatial resolution of 20 µm, and data were normalized to root mean square. GABA ions were detected in BM sections (n = 4), and both the protonated molecule ($C_4H_{10}NO_2^+$, [M + H]$^+$, *m/z* 104), as well as the dehydrated ion ($C_4H_8NO^+$, [M − H_2O + H]$^+$, *m/z* 86), were detected with high intensity in the standard and femur (Figure 2A-C; supplemental Figure 2A-B). Upon visual analysis of the IMS data, the *m/z* 86 and *m/z* 104 ions had the same spatial distribution in the samples (Figure 2B-C). In the standard, the limit of detection was between 100 µM and 1 mM GABA (Figure 2B-C). High-resolution detail from BM diaphysis (Figure 2D) shows *m/z* 86 is highly localized to the outer endosteal region.

To confirm detection of a molecule with a different spatial distribution in the BM, we used IMS to detect heme, an indicator of erythrocyte localization. Heme was at high levels within the central sinus that carries large blood volumes. Both unbound ([M + H]$^+$, *m/z* 567) and iron-bound ([M + H]$^+$,

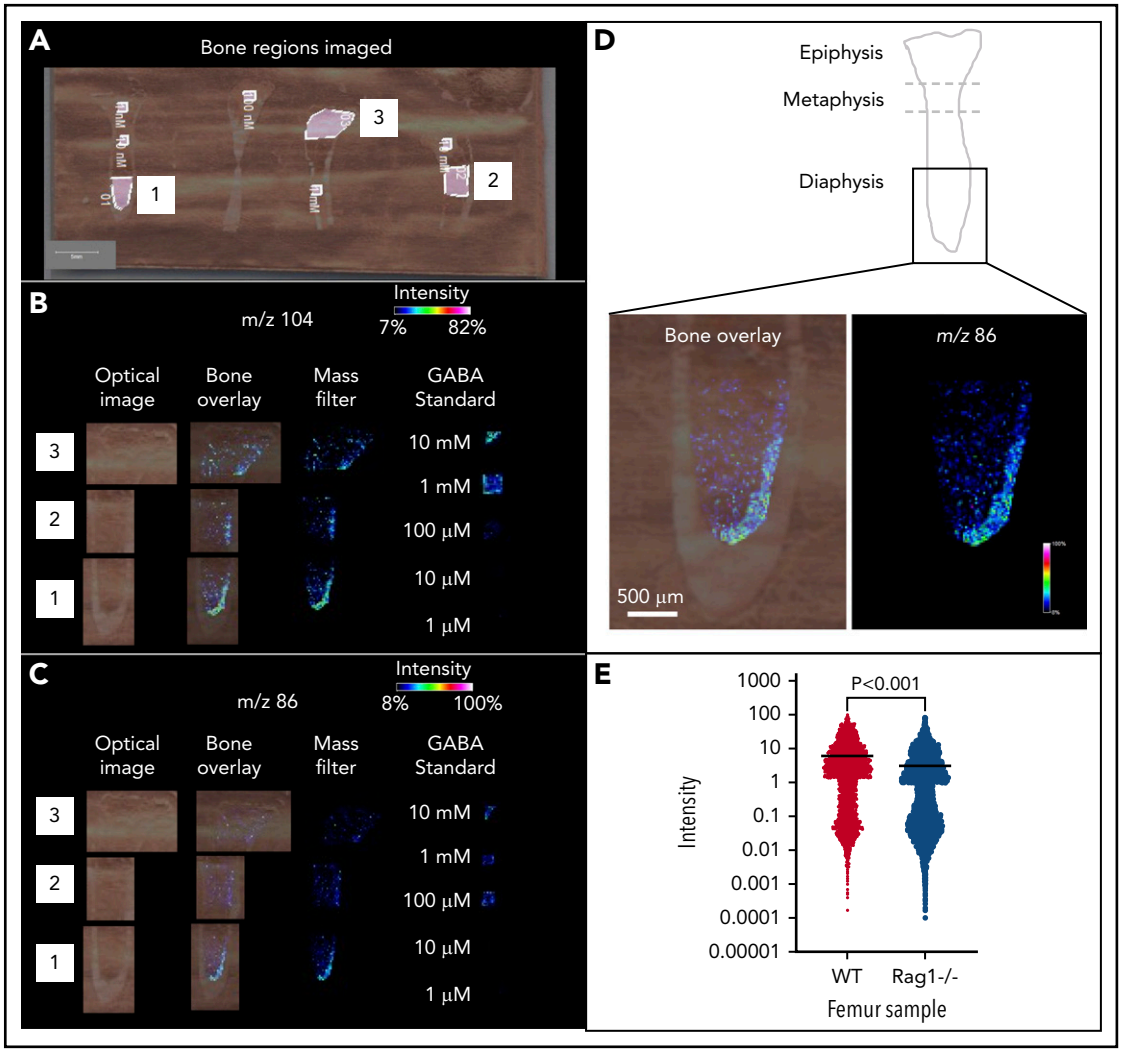

Figure 2. IMS shows GABA ion is enriched in the endosteal region of the BM. (A-C) IMS of WT bone sections (n = 2 mice). (A) "Bone regions imaged" shows slide with 3 regions selected for IMS analysis (1-3), in sum they represent an entire femur slice. The slide is spotted with commercial GABA standards. (B) Left to right, Optical images of captured regions, bone overlay of mass filter on optical image (to confirm localization to endosteum), mass filter (black background for increased visible intensity), and GABA standards (concentrations from 1 μM to 10 mM), for *m/z* 104 (adjusted intensity range between 7% [dark blue] and 82% [white]). (C) As in panel B, for *m/z* 86 (adjusted intensity range between 8% [dark blue] and 100% [white]). GABA standards show limit of detection is between 100 μM and 1 mM. (D) Detail showing endosteal enrichment of GABA signal in mass filter and bone overlay for *m/z* 86. (E) Quantification of IMS of femur sections from WT and *Rag1*$^{-/-}$ mice show a significant decrease of GABA ion in the *Rag1*$^{-/-}$ bones ($P < .001$). Error bars indicate standard deviation of data sets based on 4 measurements: 2 biological samples × 2 technical replicates per biological sample (see also supplemental Figure 2).

m/z 616) heme was detected in the central region of the BM (supplemental Figure 2E), and was distinct from endosteal localization of GABA (supplemental Figure 2F).

Following our finding that B cells express the GABA-producing enzyme Gad1, and are potential sources of GABA, we used IMS to evaluate relative contributions of B cells to GABA levels in the BM. Although IMS is not completely quantitative, the limit of detection, determined by ionization efficiency of the standard, provides a general measure of GABA amounts produced in BM. We compared GABA levels in *Rag1*$^{-/-}$ and WT femur sections. GABA levels were significantly lower in *Rag1*$^{-/-}$ B-cell–deficient bones (Figure 2E). Representative IMS data show GABA levels reduced in the endosteal region of *Rag1*$^{-/-}$ femur (supplemental Figure 2G-H).

Gabbr1-null mutants have reduced numbers of hematopoietic progenitors and B lymphocytes

Reports established a neurological phenotype in *Gabbr1* loss-of-function mouse mutants on various genetic backgrounds.[16-18] To conduct consistent hematopoietic analysis, we generated a *Gabbr1*-null (*Gabbr1*$^{-/-}$) mutant on a C57BL/6 background using CRISPR/Cas9 gene editing (supplemental Figure 3A). Guide RNAs designed to target *Gabbr1* exon 5, which is shared by all isoforms, generated a nonsense mutation due to a 1-bp adenine insertion (+1 bp [A]; supplemental Figure 3A). Mutants were undersized compared with littermates (supplemental Figure 3B) and had slightly reduced body weight (supplemental Figure 3C). We confirmed loss of Gabbr1 protein by western blot of brain tissue (supplemental Figure 3D). Our *Gabbr1*-null mutants phenocopied those previously generated

on other mutant backgrounds, as confirmed by spontaneous seizures and failure to survive beyond P20 because of neurological defects.[16-18]

Given specific expression of *Gabbr1* in a subset of HSPCs (Figure 1B-C), we analyzed BM and PB of *Gabbr1*$^{-/-}$ mutants for hematopoietic phenotype. Due to poor survival, analysis was consistently performed at P15. Characterization of LSK progenitors showed moderate but consistent (n = 9) defects in absolute numbers of BM cells of *Gabbr1*$^{-/-}$ mice (Figure 3A). No significant differences were observed in the long-term HSC (LT-HSC) population and in total BM cellularity (Figure 3A). We analyzed other populations, such as multipotent progenitor (MPP) populations MPP1-3; all showed pronounced decreases in numbers (supplemental Figure 4A). Downstream of LSKs, we observed significant decreases only in percentages and absolute numbers of CLPs (Figure 3B; supplemental Figure 4B). We analyzed BM B-cell developmental stages by Hardy fraction markers[30,31] (supplemental Figure 4C) and detected dramatic decreases in abundance of fractions B through E (supplemental Figure 4C; Figure 3E). Consistent with this, PB showed defects in white blood cells (WBCs) and lymphocytes, but not in neutrophils (Figure 3C). Flow cytometry indicated that PB B220^{+} B cells were significantly reduced, with no differences in CD4^{+} T cells, CD11b^{+} and Gr1^{+} myeloid cells (Figure 3D), or red blood cells and hemoglobin content (supplemental Figure 3E). Platelet counts were moderately decreased (supplemental Figure 3E). This indicates that loss of Gabbr1 affects abundance of LSK progenitors, without significant effects on phenotyped LT-HSCs, and that developmental defects in BM maturation of B-cell lymphocytes are the primary defects in PB.

Because our constitutive whole-body *Gabbr1*$^{-/-}$ mutants have an early hematopoietic phenotype at P15, we evaluated any hematopoietic development disruption in FL. Timed matings of *Gabbr1*$^{+/-}$ parents produced viable embryonic day 14.5 (E14.5) embryos with no apparent gross morphological phenotype (data not shown). FL analysis indicated no significant difference in the number of LSK progenitors and LT-HSCs between *Gabbr1*$^{-/-}$ and *Gabbr1*$^{+/+}$ littermates (supplemental Figure 3F). To determine whether the Gabbr1-GABA axis was present in the FL, we performed mass spectrometry to detect GABA ion in whole BM of P15 mice and the FL of E14.5 embryos. We did not detect GABA in the E14.5 FL (supplemental Figure 3G). This reveals a specific BM niche requirement for Gabbr1 not applying to development of HSPCs in FL.

Hematopoietic reconstitution potential is impaired by loss of Gabbr1

Our results suggest that hematopoietic defects in P15 *Gabbr1*$^{-/-}$ mutants are specific to phenotypic LSK progenitors, but not LT-HSCs (Figure 3A). As mutants are constitutive knockouts, their hematopoietic phenotypes could be due to Gabbr1-dependent BM niche defects. To confirm that the LSK progenitor defect is cell autonomous, and to test functionality of hematopoietic cells that lack Gabbr1 because phenotype does not always recapitulate function of HSPCs,[32] we performed direct transplantation of 1 × 10^{6} whole BM cells from *Gabbr1*$^{+/+}$ or *Gabbr1*$^{-/-}$ P15 littermates into lethally irradiated CD45.1^{+} WT recipient mice in a noncompetitive assay (supplemental Figure 5A diagrammatic representation). Reconstitution was monitored every 4 weeks posttransplant for 3 months. Within the first 4 weeks, a significant defect in total PB reconstitution was observed in the percentage of CD45.2^{+} *Gabbr1*$^{-/-}$ donor cells (supplemental Figure 5A). However, by 2 months posttransplant, CD45.2^{+} *Gabbr1*$^{-/-}$ donor cells overcame this initial deficit and fully reconstituted irradiated recipients. This suggests that the phenotype 1 month posttransplant may result from defects in short-term HSCs or progenitors, and recovery of reconstitution could be due to LT-HSCs. Thus, we repeated the transplant experiment, but instead of whole BM, used 350 sorted CD45.2^{+} LT-HSCs (LSK/CD48^{-}/CD150^{+}) from BM of P15 *Gabbr1*$^{+/+}$ or *Gabbr1*$^{-/-}$ donors, injected along with 5 × 10^{5} CD45.1/2 splenic support cells (supplemental Figure 5B). Again, CD45.1^{+} recipients transplanted with CD45.2^{+} *Gabbr1*$^{-/-}$ donor cells showed initial deficit in PB reconstitution but recovered to WT levels by 2 and 3 months after transplant (supplemental Figure 5B). Although this suggested a cell-autonomous role for Gabbr1 in hematopoietic stem and/or progenitor cells, the dynamics of reconstitution by Gabbr1-null cells was still not clear.

We hypothesized that loss of Gabbr1 in a competitive transplant would permanently affect hematopoietic recovery because it would test the fitness and ability of Gabbr1-null LT-HSCs to compete for the same niche with WT LT-HSCs. We transplanted 350 sorted LT-HSCs, harvested from BM of *Gabbr1*$^{+/+}$ or *Gabbr1*$^{-/-}$ littermates, in competition with 350 BM LT-HSCs from a CD45.1/.2 donor, along with CD45.1 splenic support cells (Figure 4A diagrammatic representation). In this competitive setting, defects in *Gabbr1*$^{-/-}$ PB reconstitution persisted for 3 months, confirming lack of *Gabbr1*$^{-/-}$ cell fitness (Figure 4B). Interestingly, lineage contributions of transplanted *Gabbr1*$^{-/-}$ HSCs to PB were reduced in lymphoid, but not myeloid, compartments (supplemental Figure 5C). Numbers of *Gabbr1*$^{-/-}$ BM CD45.2^{+} LSK progenitors and LT-HSCs were significantly reduced at 3 months (Figure 4C), as were several progenitor populations (supplemental Figure 5D).

To determine the extent of the competitive reconstitution defect, we performed secondary transplants with either 1 × 10^{6} whole BM cells harvested from primary competitive recipients (supplemental Figure 5E), or by sorting 350 CD45.2^{+} LT-HSCs derived from primary recipient BM, and initiating a secondary competition with 350 HSCs from a CD45.1/.2 donor (Figure 4D). In whole BM secondary competitive transplant, the ratio of WT to *Gabbr1*$^{-/-}$ reconstitution was maintained, demonstrating that these defects were in a self-renewing HSC population (supplemental Figure 5E); terminal analysis revealed dramatic decreases in the percentage of LSK progenitors and LT-HSCs (supplemental Figure 5F). Secondary competitive transplant with 350 sorted *Gabbr1*$^{-/-}$ LT-HSCs also showed significant defects in reconstitution (Figure 4D). At the terminal 4-month time point, BM analysis of the recipients indicated decreased overall *Gabbr1*$^{-/-}$ cellularity and significant defects in LSK progenitors and LT-HSC frequency (Figure 4E). In both cases, reconstitution defects persisted up to 4 months after secondary transplants. These results support our hypothesis that there is a cell-autonomous role for GABBR1 in hematopoietic reconstitution, and in HSPC competitive fitness.

Proliferative capacity of the HSPC pool in *Gabbr1*$^{-/-}$ mutants is reduced

To understand Gabbr1 signaling in HSPCs, we performed cell-cycle and apoptotic assays in phenotypic populations of BM LSK

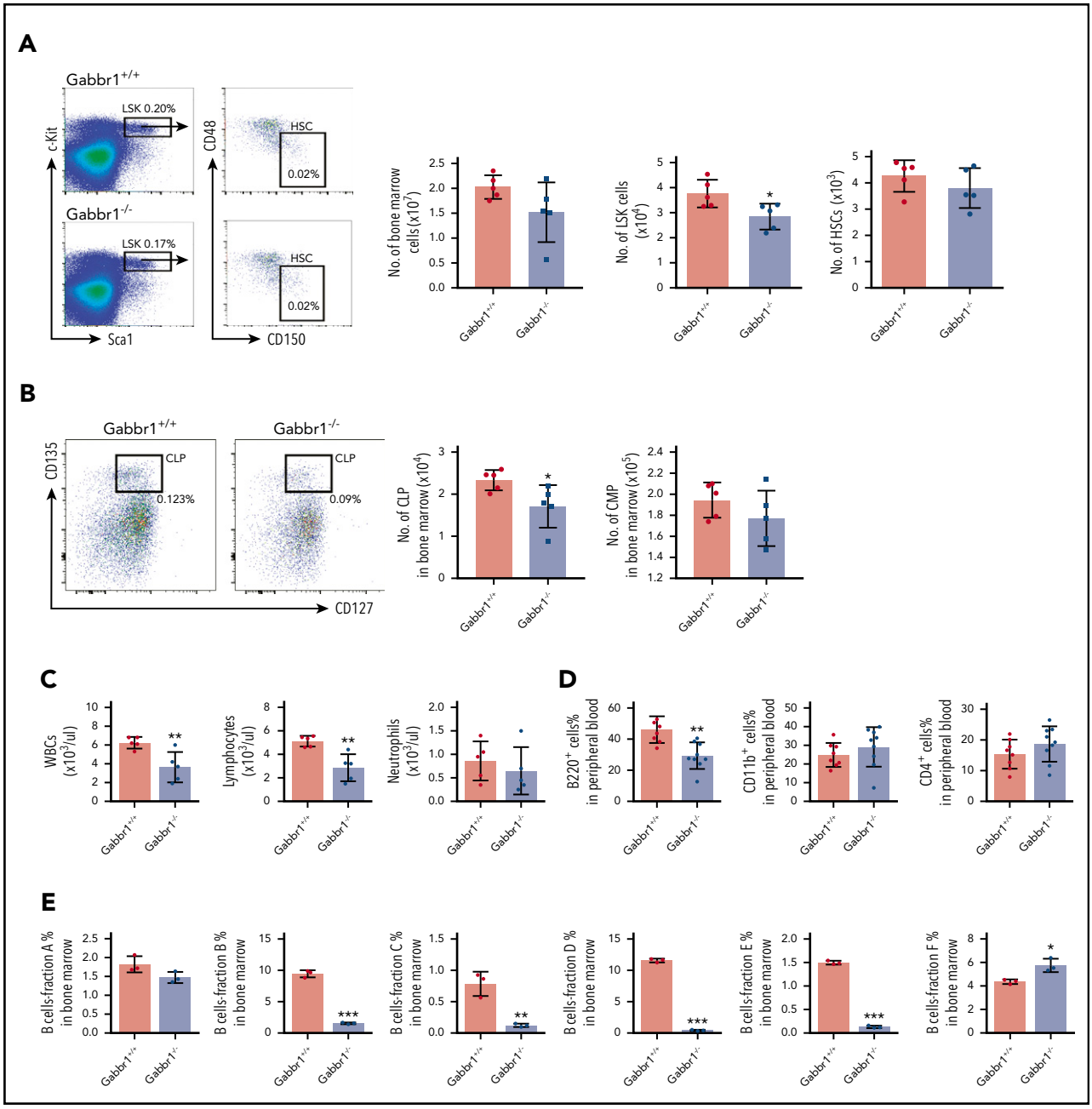

Figure 3. *Gabbr1*$^{-/-}$ mutants have decreased numbers of LSK progenitors in BM and lymphocytes in PB. (A) Left panel, Representative flow cytometry gates. Right panels, There are comparable numbers of total BM cells from 2 femur and 2 tibias. The number of LSK progenitors, but not HSCs (LSK/CD48$^-$/CD150$^+$), is reduced in *Gabbr1*$^{-/-}$ BM (n = 5 WT vs n = 5 mutants). (B) Left panel, Representative flow cytometry gates for CLP. Right panels, The number of Lin$^-$Sca1^{low}cKit^{low}CD135^{high}CD127^{low} (CLP) progenitors, but not CMP (Lin$^-$Sca1$^-$cKit$^+$CD34^{high}CD16/32^{low}), is reduced in *Gabbr1*$^{-/-}$ BM (n = 5 WT vs n = 5 mutants). (C) WBCs and lymphocytes, but not neutrophils, were reduced in *Gabbr1*$^{-/-}$ PB (n = 5 WT vs n = 5 mutants). (D) Percentages of B220$^+$, but not CD11b$^+$ or Gr-1$^+$, cells were reduced in *Gabbr1*$^{-/-}$ PB (n = 8 WT vs n = 9 mutants). (E) The analysis of Hardy B-cell fractions in the BM from Gabbr1$^{+/+}$ and Gabbr1$^{-/-}$ mice (n = 3 WT vs n = 3 mutants). Data are represented as mean plus or minus standard deviation (SD) (*$P < .05$; **$P < .01$; ***$P < .001$). Analyses performed at P15 (see also supplemental Figures 3 and 4).

progenitors of WT and *Gabbr1*$^{-/-}$ P15 littermates. Ki-67 and 7-aminoactinomycin D (7-AAD) counterstaining determined LSK progenitor cell-cycle progression. Flow cytometry for quantification of the LSK cell cycle indicated significant defects in *Gabbr1*$^{-/-}$ LSKs during cell growth and entry into G1 phase (Figure 5A). However, proapoptotic analysis by annexin V staining or caspase 3 activity of LSK progenitors and HSCs in the BM showed no difference between *Gabbr1*$^{+/+}$ and *Gabbr1*$^{-/-}$ P15 littermates (supplemental Figure 6A-B).

Phenotypic analysis of HSPCs confirms their presence, but it does not allow assessment of functional characteristics of these cells (eg, their proliferative and differentiation capacity). For functional progenitor capacities, CFU assays are used. This allows one to determine proliferative capacity, and the percentage of specific progenitor cell types (CFU granulocyte macrophage [CFU-GM], burst-forming unit erythroid [BFU-E], and CFU granulocyte, erythroid, macrophage, megakaryocyte [CFU-GEMM]) in S-phase of the cell cycle (cycling rate) by using a

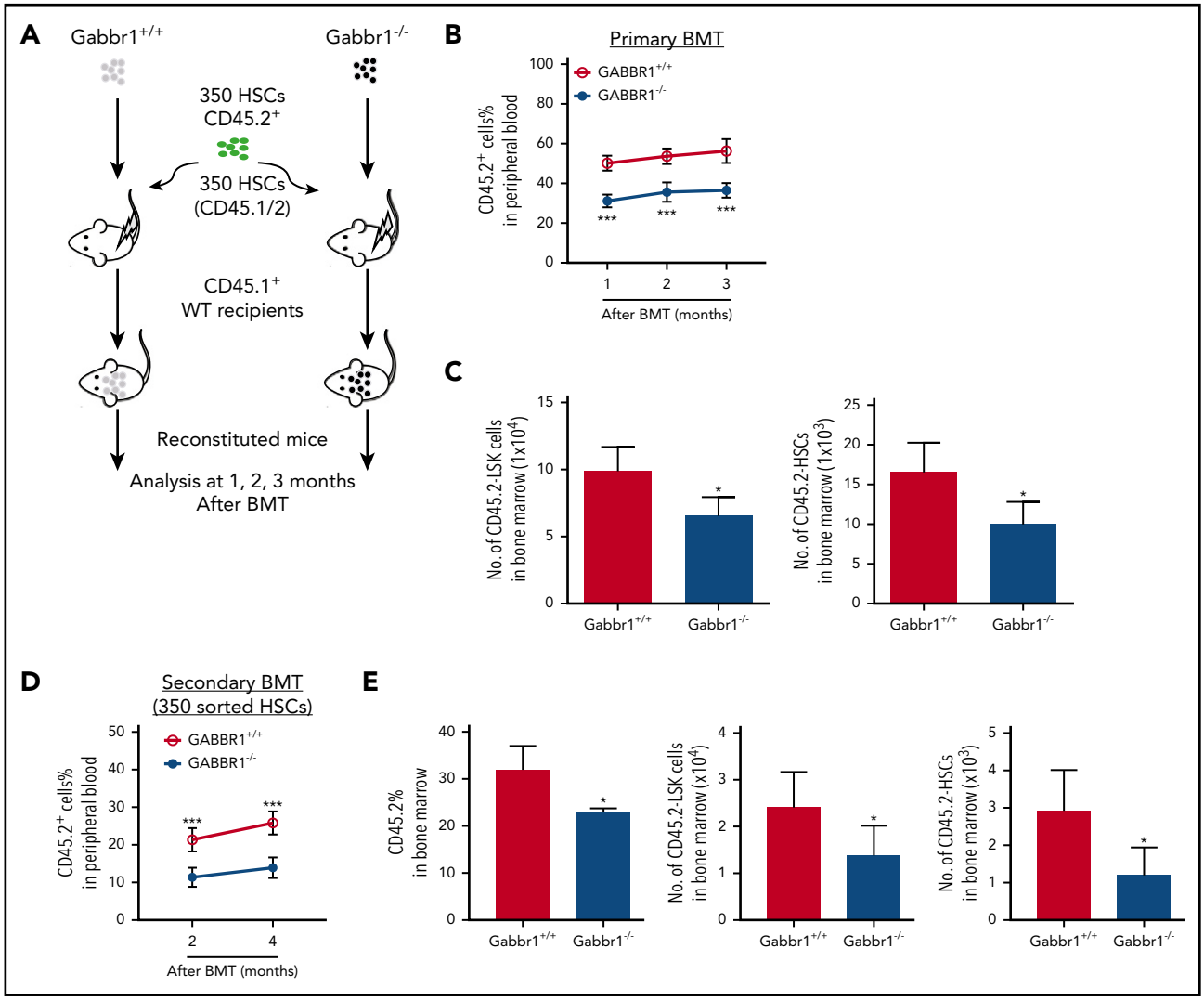

Figure 4. *Gabbr1*$^{-/-}$ mutant HSCs have reduced engraftment ability in competitive transplants. (A-C) Primary competitive BM transplantation (BMT). (A) Three hundred fifty HSCs from WT and *Gabbr1*$^{-/-}$ mice were sorted and transplanted into irradiated CD45.1 recipients, together with 350 HSCs from CD45.1/2 mice. (B) Mice were analyzed for reconstitution of PB with donor-derived CD45.2 cells at 1, 2, and 3 months posttransplant. (C) Three months posttransplant, BM CD45.2^{+} LSK progenitors and HSCs were still reduced (n = 5 recipients per group). (D-E) Secondary transplantation. Three hundred fifty WT or *Gabbr1*$^{-/-}$ mutant HSCs from primary recipient mice were sorted and transplanted into irradiated CD45.1 recipients, together with 350 sorted HSCs from CD45.1/2 mice. (D) Mice were analyzed for reconstitution of PB with donor-derived CD45.2 cells at 1, 2, and 3 months posttransplant for donor reconstitution. (E) Three months postsecondary transplant, BM CD45.2^{+} LSK progenitors and HSCs were still reduced (n = 5 recipients per group). Data are presented as mean plus or minus SD. (WT vs *Gabbr1*$^{-/-}$ mice: *$P < .05$; **$P < .01$; ***$P < .001$) (see also supplemental Figure 5).

well-established high specific activity tritiated thymidine cell-kill procedure.[33-37] We evaluated functional BM progenitors CFU-GM, BFU-E, and CFU-GEMM of *Gabbr1*$^{+/+}$ and *Gabbr1*$^{-/-}$ littermate mice (P13-15). Absolute numbers of BM CFU-GM in *Gabbr1*$^{-/-}$ mice were significantly decreased compared with *Gabbr1*$^{+/+}$ BM (Figure 5B). Almost all *Gabbr1*$^{-/-}$ progenitors were in a slow or noncycling state (Figure 5C). No differences in size or appearance of colonies were noted.

To understand proliferation defects in *Gabbr1*$^{-/-}$ mutant HSPCs, we used a bioinformatics approach to find common characteristics among subsets of HSPCs expressing *Gabbr1* (Figure 1B). We performed gene-set enrichment analysis[38] based on ranked correlation of coexpressed genes from previously published single HSPC RNA-seq data.[22] Four of the top 10 gene-ontology annotations that correlated positively with *Gabbr1* expression were associated with type I or II interferon signaling (supplemental Figure 7; supplemental Tables 2 and 3). To test in vivo the prediction that Gabbr1 is involved in type I interferon response, a known regulator of HSPC proliferation,[39] we treated WT and *Gabbr1*$^{-/-}$ P15 littermates with an intraperitoneal injection of polyinosinic: polycytidylic acid [poly(I:C)]. BM analysis of WT and *Gabbr1*$^{-/-}$ littermates 48 hours after poly(I:C) injection indicated significant decreases in numbers of *Gabbr1*$^{-/-}$ progenitors; Ki-67 and 7-AAD cell-cycle analysis further confirmed a G1-entry defect in *Gabbr1*$^{-/-}$ progenitors (Figure 5D). Poly(I:C) treatment had no effect on the proapoptotic status of *Gabbr1*$^{-/-}$ LSK progenitors (supplemental Figure 6C). To determine whether G1-entry defects in LSK progenitors continued to affect *Gabbr1*$^{-/-}$ mutants during S-phase, we injected 5-bromo-2′-deoxyuridine (BrdU) intraperitoneally in P15 WT and *Gabbr1*$^{-/-}$ littermates and analyzed BrdU incorporation by flow cytometry in LSK

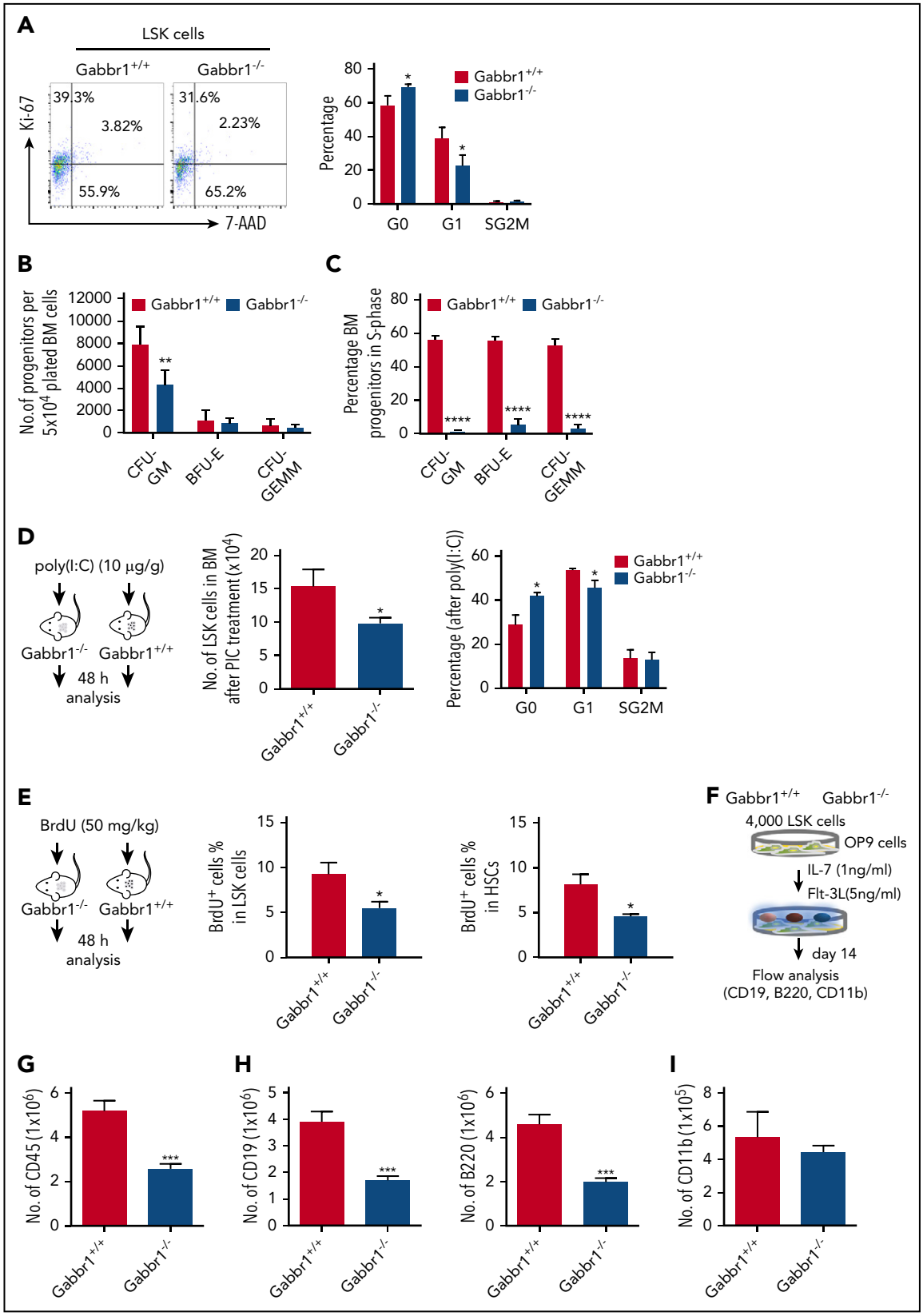

Figure 5. The *Gabbr1*$^{-/-}$ mutant HSPC pool has reduced proliferative capacity. (A) Cell-cycle analysis. Left panel, Representative flow cytometry gates of cell-cycle analysis by Ki-67 and 7-AAD in LSK progenitors. Right panel, There are more cells in G0 phase in *Gabbr1*$^{-/-}$ LSK progenitors when compared with *Gabbr1*$^{+/+}$ controls (n = 6 per group). (B-C) CFU assays were performed to determine proliferative and differentiative capacity of HSPCs. (B) Absolute numbers of progenitors were determined by plating equal numbers of BM (5×10^4 cells) from WT or *Gabbr1*$^{-/-}$ tibias. (C) The tritiated thymidine incorporation assay was used to determine the cell-cycling status of BM progenitors. (D) Stimulation with poly(I:C) (10 μg/g) was done by intraperitoneal injection into WT and *Gabbr1*$^{-/-}$ mice (n = 4 per group). Forty-eight hours later, LSK progenitor number and cell

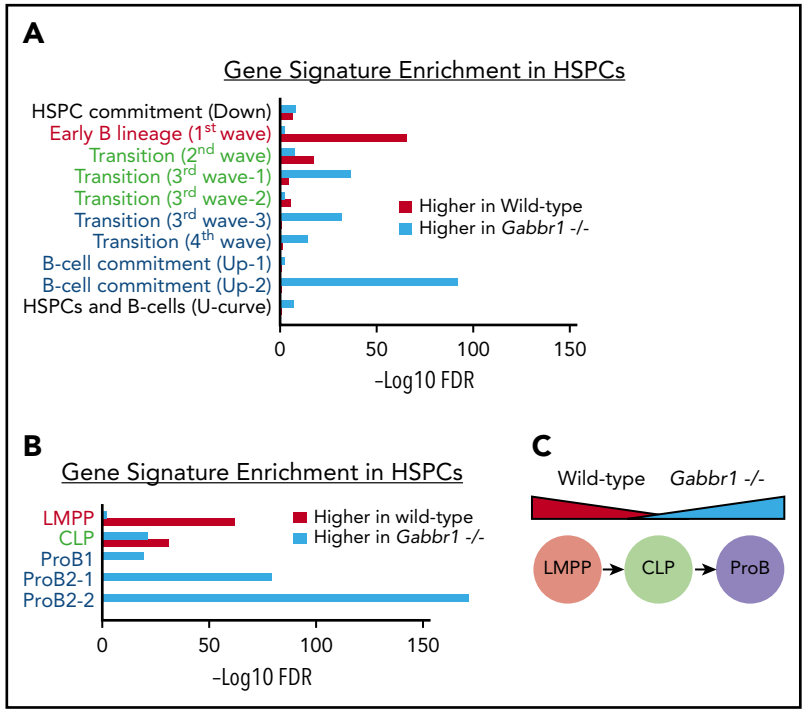

Figure 6. Gene-signature analysis shows a shift in pooled RNA-seq expression profiles from a progenitor-like state in WT HSPCs to pro–B-cell commitment in *Gabbr1*$^{-/-}$ mutant HSPCs. Gene signatures are defined by data from Miyai et al,[42] and false discovery rate (FDR) of gene-signature enrichment is shown as red bars for WT HSPCs and turquoise bars for *Gabbr1*$^{-/-}$ mutant HSPCs. (A) Gene signatures from in vitro B-cell differentiation show a progressive shift from early B-lineage markers in WT HSPCs (red text), to a mix of signatures in "transition" stage (green text), and finally to pro–B-cell commitment signatures in *Gabbr1*$^{-/-}$ mutant HSPCs (blue text). (B) This same pattern is mirrored in the gene signatures of sorted LMPPs, CLPs, and pro-B cells. (C) Diagram showing the shift in expression profiles between WT and *Gabbr1*$^{-/-}$ mutant HSPCs.

progenitors and long-term HSCs 48 hours later. For both populations, significant decreases in BrdU incorporation were observed (Figure 5E), confirming defects in proliferative capacity of phenotypically defined *Gabbr1*$^{-/-}$ hematopoietic progenitors and stem cells.

Differentiation of *Gabbr1*$^{-/-}$ mutant progenitors in vitro reveals proliferation defects in B-cell lineages

To directly test whether loss of Gabbr1 affects overall proliferation of progenitors, or whether it has specific consequences in lineage commitment, we used OP9 stromal cells for lymphoid and myeloid differentiation of sorted BM progenitors. Using previously described OP9 conditions,[40] we differentiated 4000 LSK progenitors from P15 *Gabbr1*$^{-/-}$ or *Gabbr1*$^{+/+}$ littermates into myeloid or B-cell lymphoid lineages (Figure 5F). After 2 weeks, overall cellular content and phenotypic analysis of differentiated lineages were conducted. Results indicated decreased overall numbers of CD45^{+} cells produced by *Gabbr1*$^{-/-}$ LSK progenitors (Figure 5G), in accordance with in vivo analysis of proliferation defects in the mutants. Furthermore, a significant defect in B-cell lineage development was indicated by reduced CD19^{+} and B220^{+} cells originating from *Gabbr1*$^{-/-}$ mutants (Figure 5H). No defect was detected in the myeloid compartment as indicated by presence of CD11b^{+} cells (Figure 5I). This was confirmed by repeating differentiation assays and supplementing promyeloid cytokines interleukin-3 and interleukin-6 in our OP9 differentiation media. There was no significant difference in expanded myeloid compartments between WT and *Gabbr1*$^{-/-}$ mutant progenitors (supplemental Figure 6D). Overall, this supports our in vivo analysis of *Gabbr1*$^{-/-}$ mutants by confirming defects in progenitor proliferation, and in B-cell differentiation.

B-cell program genes are dysregulated in *Gabbr1*$^{-/-}$ mutant HSPCs

To better understand molecular phenotypes of *Gabbr1*$^{-/-}$ mutant HSPCs, we sorted and pooled ~12 000 LSKs from *Gabbr1*$^{+/+}$ or *Gabbr1*$^{-/-}$ P15 BM for bulk RNA-seq analysis. After initial comparison of differentially expressed genes between WT and mutant LSKs, and Ingenuity Pathway Analysis,[41] we observed significant increases in expression of genes associated with B-cell development in mutant LSKs (ratio = 0.33; −log(B-H *P* value) = 8.69; supplemental Table 4). To further investigate these changes, we used a recently published "blueprint" for B-cell development to generate custom gene sets.[42] These sets were associated with progressive stages of in vitro MPP differentiation into B lymphocytes (Figure 6A), or sorted BM populations of phenotypically defined lymphoid-primed MPPs (LMPPs), CLP, and pro-B cells (Figure 6B). Gene signatures from the first and earliest stages of B-lineage differentiation (Figure 6A), or sorted LMPPs (Figure 6B), were significantly enriched in WT HSPCs compared with *Gabbr1*$^{-/-}$ HSPCs; alternatively, this could be interpreted as downregulation of early progenitor-associated genes in mutant HSPCs. The second stage of B-cell differentiation or "transition"[42] is similar to a CLP.

Figure 5 (continued) cycle were analyzed. (E) BrdU incorporation assay. BrdU (50 mg/kg) was intraperitoneal injected into WT (n = 6) and *Gabbr1*$^{-/-}$ mice (n = 5). Forty-eight hours later, percentages of BrdU^{+} cells in LSK and LSK CD48^{-} progenitor populations were analyzed. (F-I) In vitro B-cell differentiation assay. (F) Experimental design. Four thousand sorted LSK progenitors from WT and *Gabbr1*$^{-/-}$ mice were seeded onto OP9 cells. After 1 week, cells were passaged onto fresh OP9 cells. At day 14, all cells were collected, counted, and stained with CD45 (G), CD19 (H; left panel), B220 (H; right panel), and CD11b (I) antibodies. The absolute numbers were presented as mean plus or minus SD (data were from 2 independent experiments with 4-5 replicates.). **P* < .05; ***P* < .02; ****P* < .001; *****P* = 0 vs *Gabbr1*$^{+/+}$ controls. Analyses of panels A and D-I performed at P15; panels B and C performed at P13 and P15 (see also supplemental Figure 6).

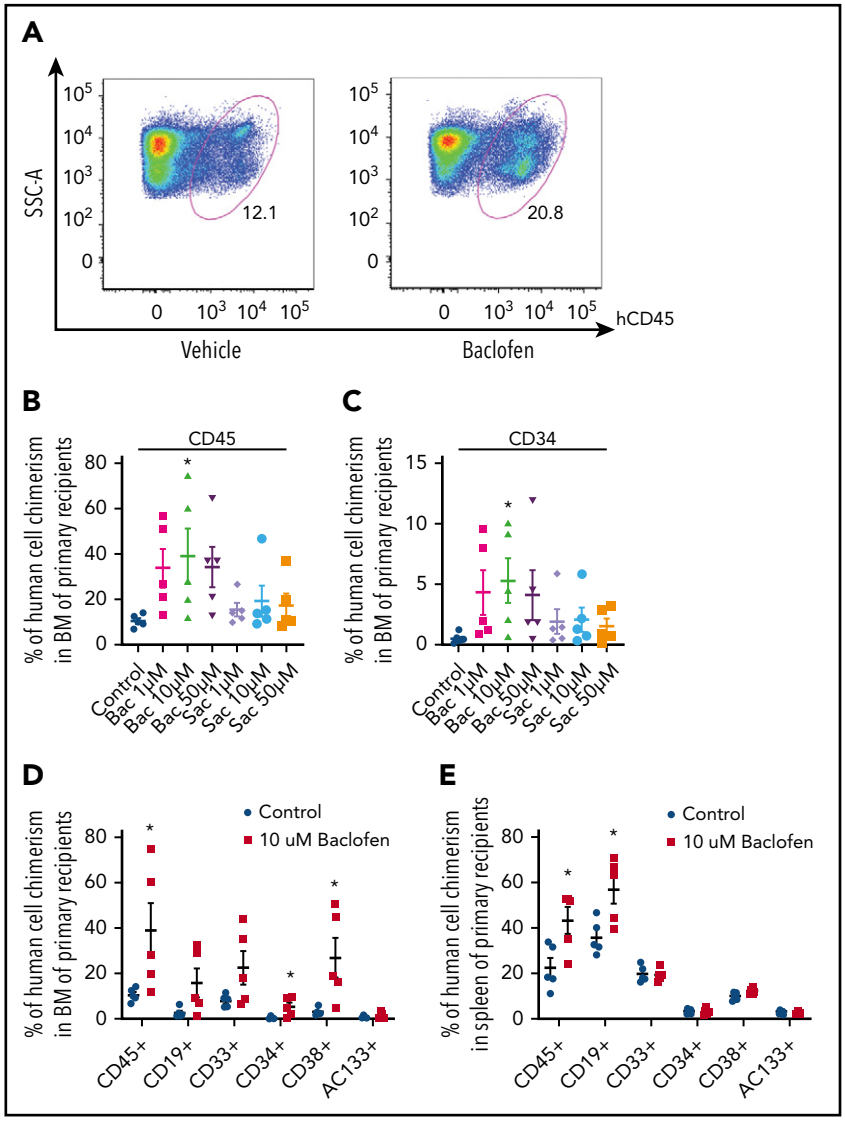

Figure 7. The GABBR1 agonist baclofen increases long-term engraftment of human UCB HSPCs. (A) Representative flow cytometry analysis of immunodeficient mouse BM 16 weeks after transplantation with human UCB HSPCs after treatment with vehicle (left) or GABBR1 agonist baclofen (right). Results show percentage engraftment of human CD45$^+$ cells (hCD45). (B-C) Dose-dependent engraftment of human hematopoietic CD45$^+$ cells (A), and CD34$^+$ HSPCs (B). Compared with vehicle controls, the most effective dose is 10 μM baclofen. The GABBR1 antagonist 2-hydroxy-saclofen does not significantly increase engraftment. (D-E) Comparison of engraftment percentage of various hematopoietic populations in BM (D), and spleen (E), at the optimal dose of 10 μM baclofen (red) compared with vehicle control (blue) (n = 5 per group; Student *t* test; **P* < .05; mean = standard error of the mean [SEM]) (see also supplemental Figure 8). Bac, baclofen; Sac, 2-hydroxy-saclofen; SSC-A, side scatter area.

This gene signature is mixed, with some representative genes enriched in WT, and some in *Gabbr1*$^{-/-}$ mutant HSPCs (Figure 6A-B). Later-stage B-cell commitment and pro-B-cell gene signatures[42] are very highly enriched in *Gabbr1*$^{-/-}$ mutant HSPCs (Figure 6A-B). This demonstrates significant shifts in expression profiles of LSK HSPCs from early, progenitor-like signatures to that of committed pro-B cells (Figure 6C), suggesting that Gabbr1 plays a role in differentiation of HSPCs to B-lineage cells.

Brief treatment with GABBR1 agonist increases long-term engraftment of human UCB HSPCs

Findings from our mouse model indicated a role for the Gabbr1 neuroreceptor in 2 aspects of hematopoiesis: proliferation of HSPCs and differentiation of B-lineage cells. To evaluate functional conservation of Gabbr1 in hematopoiesis, and translational potential of GABA signaling for HSPCs, we exposed CD34$^+$ UCB cells for 2 hours in vitro with increasing doses of either baclofen, a clinically approved GABA agonist,[43] or 2-hydroxy-saclofen, a selective antagonist of GABA B receptor.[44] After treatment, cells were injected IV into sublethally irradiated NOD-*scid.Il2rg*^{null} (NSG) recipients, and xenograft outcome was assayed 16 weeks later. Treatment with 10 μM baclofen showed dramatic enhancement over vehicle control in engraftment of hCD45$^+$ cells in NSG recipients (Figure 7A). At 16 weeks, total human blood CD45$^+$ (Figure 7B) and progenitor-specific CD34$^+$ (Figure 7C) BM engraftment in NSG mice exhibited a trend to increase after agonist treatment, and a significant improvement after 10 μM baclofen. 2-hydroxy-saclofen treatment did not significantly increase engraftment at any of the tested doses. Further lineage analysis of BM chimerism in vehicle control and 10 μM baclofen treatment revealed significant increases in overall engraftment (CD45$^+$), and in progenitor engraftment (CD34$^+$ and CD38$^+$; Figure 7D). In the spleen of transplanted NSG mice, this pattern persisted with significant increases in overall engraftment, and a near twofold enhancement in CD19$^+$ B-cell reconstitution (Figure 7E). At 16 weeks posttransplantation, CFU assays indicated that progenitor colonies in the BM derived from NSG mice transplanted with baclofen-treated CD34$^+$ UCB cells were threefold higher than controls (supplemental Figure 8B). Interestingly, CD34$^+$ UCB cells analyzed for in vitro CFUs after a 2-hour treatment, baclofen did not produce increased colonies, suggesting that conditions in vivo are required for a sustained increase in progenitor numbers (supplemental Figure 8A). This

supports our conclusions that Gabbr1-mediated HSPC signaling promotes engraftment, reconstitution potential, and differentiation of the B-cell lineage.

Discussion

It has been known that human HSPCs express neurotransmitter receptors. However, their function in vivo has remained enigmatic. We studied the role of GABA B type receptor Gabbr1, expressed in a subset of HSPCs, in a loss-of-function mouse model. In steady state, *Gabbr1*$^{-/-}$ mutants have reduced MPP and LSK progenitors, as well as WBCs, lymphocytes, and B cells. This specific role for *Gabbr1* in B-cell development was further highlighted by custom gene-signature analysis.[42] Although we were directly comparing the expression profiles of phenotypic LSK progenitors isolated from WT and *Gabbr1*$^{-/-}$ mutants, we observed a significant change from the expected MPP gene signature, indicating a dysregulation of B-cell differentiation in HSPCs. Analysis of developing B cells in the BM (Hardy fractions) showed dramatic reduction in B-cell maturation. This specific defect in B-lineage potential was confirmed by in vitro differentiation of *Gabbr1*$^{-/-}$ mutant LSK progenitors. We showed a premature transcriptional B-cell program in Gabbr1$^{-/-}$ HSPCs, which, when combined with a pronounced defect starting as early as Hardy fraction B, suggest that loss of Gabbr1 signaling causes loss of immature B cells in the BM. Decreases in peripheral WBCs and B cells likely result from removal of highly autoreactive B cells during the pre–B-cell receptor central tolerance checkpoint.[45]

Transplanted HSPCs from *Gabbr1*$^{-/-}$ mutants had reduced proliferative capacity and competed poorly against WT HSPCs in a competitive transplant setting. Gene-set enrichment analysis found that the single-cell expression profile of *Gabbr1*-expressing HSPCs (ie, the gene set that positively correlated with *Gabbr1* expression) was enriched for interferon pathway genes. Consistent with this finding, HSPC proliferation was reduced in *Gabbr1*$^{-/-}$ mutants after poly(I:C) treatment, suggesting a defective type I interferon response. Conversely, a brief ex vivo treatment of human UCB CD34^{+} cells with clinically approved GABA agonist, baclofen, enhanced engraftment and reconstitution of hematopoiesis in xenotransplant models.

A decrease in HSPC proliferation and function along with early defects in B-cell development indicate a unique, lineage-specific role for Gabbr1 signaling in the BM niche. IMS analysis indicated that GABA was present in the endosteal region of the BM. To better identify the cells responsible for production of GABA in the BM, we analyzed several cell types for the expression of GAD1, the enzyme required for GABA production. We showed messenger RNA and protein expression levels of GAD1 to be high in B cells. In the context of the phenotype of *Gabbr1*$^{-/-}$ mice, this indicates an intricate connection between GABA production by BM B cells with proliferation and differentiation of HSPCs. Because CLP and immature B-cell compartments are severely affected by Gabbr1 loss, this suggests a possible instructive feedback loop of GABA-Gabbr1 signaling in early B-lymphoid development.

Overall, there is still little known about GABA signaling in hematopoiesis and multilineage differentiation. Recently, a GABA A type receptor Rho 1 subunit GABRR1 was found to be expressed in HSCs and megakaryocyte progenitors,[19] and played a conserved role in platelet production. Taken together with our current study, there appears to be a complex role for GABA signaling in multiple hematopoietic lineages that act via different receptors, with GABA A type receptor Rho 1 subunit GABRR1 regulating megakaryocyte progenitors, and GABA B type receptor GABBR1 regulating HSPC numbers and B-cell differentiation. Studies in *Drosophila* and bony fish showed that GABA signaling regulates hematopoietic progenitors, suggesting an ancient and deeply conserved role in hematopoiesis.[46,47] Interestingly, genome-wide association studies have identified a rare variant in the GABBR1 locus that produces a change in WBC and lymphocyte counts.[48,49] Although further mechanistic investigation is required to fully determine the role of neurotransmitter signaling in BM HSPC populations, our ex vivo findings suggest a potential direct translational application for activation of GABA signaling in enhancing engraftment during clinical transplant.

Acknowledgments

The authors thank Linda Degenstein and the Transgenic Mouse and Embryonic Stem Cell Facility at the University of Chicago for generation of the mouse model, Maureen Regan and Brad Merrill of the University of Illinois at Chicago Genome Editing Core for CRISPR/Cas9 design and reagents, Wendy Shao and Balaji Ganesh of the University of Illinois at Chicago Flow Cytometry Core for cell sorting, Katherine Gruner and Marc Deheeger of the Mouse Histology and Phenotyping Laboratory at Northwestern University for histology, Cece Countryman and Zarema Arbieva at the University of Illinois at Chicago Core Genomics Facility for sequencing, Haley Engle and Sweta Soni for maintaining the mouse colony, and Melissa Trowbridge and Kathy Coy at Indiana University for their expert technical assistance with xenotransplant studies.

RNA-seq data analysis was performed by Pinal Kanabar and Mark Maienschein-Cline at the UIC Research Informatics Core, supported in part by the National Institutes of Health (NIH) National Center for Advancing Translational Sciences through grant UL1TR002003. Xenotransplants were conducted by core facilities funded through the Cooperative Centers of Excellence in Hematology (NIH National Institute of Diabetes and Digestive and Kidney Diseases U54DK106846) and the Indiana University Simon Comprehensive Cancer Center (NIH National Cancer Institute P30 CA082709). Research reported in this publication was supported by: the NIH National Heart, Lung, and Blood Institute (R01HL142998 [O.J.T.], R01HL134971 [K.V.P.], R35HL139599 [H.E.B.]), the NIH National Institute of Diabetes and Digestive and Kidney Diseases (K01DK103908 [O.J.T.], R01DK109188 [H.E.B.], U54DK106846 [K.E.P. and H.E.B.]), the NIH National Cancer Institute (F31CA236237 [K.E.Z.]), the NIH National Institute of General Medical Sciences (R01GM125943 [L.M.S.]), and an American Society of Hematology (ASH) Junior Faculty Scholar Award (O.J.T.). Funding was also provided by the Chicago Biomedical Consortium Catalyst Grant with support from the Searle Funds at The Chicago Community Trust (C-076 [L.M.S.]) and University of Illinois at Chicago Startup Funds (L.M.S., O.J.T., K.V.P.). B.J.C. was supported by a Tier II Canada Research Chair.

Authorship

Contribution: K.V.P. and O.J.T. conceptualized the study; K.E.P., A.L.S., B.J.B., E.C.S., S.H.C., H.E.B., K.V.P., and O.J.T. developed the study methodology; L.S., A.E.-B., K.E.Z., K.E.P., A.L.S., and E.C.S. validated the study and conducted investigations; L.S., A.E.-B., K.E.Z., B.J.C., K.E.P., A.L.S., B.J.B., and E.C.S. provided formal analysis; K.V.P., L.S., and A.E.-B. prepared and wrote the original draft; K.V.P., O.J.T., K.E.P., and H.E.B. prepared, reviewed, and edited the manuscript; L.S., K.E.Z., E.C.S., and O.J.T. prepared and visualized the study; K.E.P., L.M.S., H.E.B., K.V.P., and O.J.T. supervised the study; and L.M.S., H.E.B., K.V.P., and O.J.T. acquired funding.

Conflict-of-interest disclosure: The authors declare no competing financial interests.

ORCID profiles: A.E.-B., 0000-0002-7066-7666; L.M.S., 0000-0001-9223-7977; K.E.P., 0000-0001-6031-5707; O.J.T., 0000-0001-9146-4860.

Correspondence: Kostandin V. Pajcini, Department of Pharmacology, University of Illinois at Chicago, 909 S. Wolcott Ave, Chicago, IL 60612; e-mail: kvp@uic.edu; and Owen J. Tamplin, Department of Cell and Regenerative Biology, School of Medicine and Public Health, University of Wisconsin-Madison, 1111 Highland Ave, Madison, WI 53705; e-mail: tamplin@wisc.edu.

Footnotes

Submitted 6 December 2019; accepted 16 August 2020; prepublished online on *Blood* First Edition 3 September 2020. DOI 10.1182/blood.2019004415.

*L.S. and A.E.-B. contributed equally to this work.

†K.V.P. and O.J.T. are joint corresponding authors.

The data reported in this article have been deposited in the Gene Expression Omnibus database (accession number GSE157352).

For original data or reagents, please contact tamplin@wisc.edu or kvp@uic.edu.

The online version of this article contains a data supplement.

There is a *Blood* Commentary on this article in this issue.

The publication costs of this article were defrayed in part by page charge payment. Therefore, and solely to indicate this fact, this article is hereby marked "advertisement" in accordance with 18 USC section 1734.

REFERENCES

1. Orkin SH, Zon LI. Hematopoiesis: an evolving paradigm for stem cell biology. *Cell*. 2008; 132(4):631-644.
2. Wei Q, Frenette PS. Niches for hematopoietic stem cells and their progeny. *Immunity*. 2018; 48(4):632-648.
3. Agarwala S, Tamplin OJ. Neural crossroads in the hematopoietic stem cell niche. *Trends Cell Biol*. 2018;28(12):987-998.
4. Méndez-Ferrer S, Lucas D, Battista M, Frenette PS. Haematopoietic stem cell release is regulated by circadian oscillations. *Nature*. 2008;452(7186):442-447.
5. Steidl U, Bork S, Schaub S, et al. Primary human CD34+ hematopoietic stem and progenitor cells express functionally active receptors of neuromediators. *Blood*. 2004; 104(1):81-88.
6. Spiegel A, Shivtiel S, Kalinkovich A, et al. Catecholaminergic neurotransmitters regulate migration and repopulation of immature human CD34+ cells through Wnt signaling. *Nat Immunol*. 2007;8(10):1123-1131.
7. Kalinkovich A, Spiegel A, Shivtiel S, et al. Blood-forming stem cells are nervous: direct and indirect regulation of immature human CD34+ cells by the nervous system. *Brain Behav Immun*. 2009;23(8):1059-1065.
8. Cosentino M, Marino F, Maestroni GJM. Sympathoadrenergic modulation of hematopoiesis: a review of available evidence and of therapeutic perspectives. *Front Cell Neurosci*. 2015;9:302.
9. Kwan W, Cortes M, Frost I, et al. The central nervous system regulates embryonic HSPC production via stress-responsive glucocorticoid receptor signaling. *Cell Stem Cell*. 2016; 19(3):370-382.
10. Goolsby J, Marty MC, Heletz D, et al. Hematopoietic progenitors express neural genes. *Proc Natl Acad Sci USA*. 2003;100(25): 14926-14931.
11. Xu C, Zhang W, Rondard P, Pin JP, Liu J. Complex GABAB receptor complexes: how to generate multiple functionally distinct units from a single receptor. *Front Pharmacol*. 2014; 5:12.
12. Chapman RW, Hey JA, Rizzo CA, Bolser DC. GABAB receptors in the lung. *Trends Pharmacol Sci*. 1993;14(1):26-29.
13. Calver AR, Medhurst AD, Robbins MJ, et al. The expression of GABA(B1) and GABA(B2) receptor subunits in the cNS differs from that in peripheral tissues. *Neuroscience*. 2000; 100(1):155-170.
14. Zangiacomi V, Balon N, Maddens S, Tiberghien P, Versaux-Botteri C, Deschaseaux F. Human cord blood-derived hematopoietic and neural-like stem/progenitor cells are attracted by the neurotransmitter GABA. *Stem Cells Dev*. 2009;18(9):1369-1378.
15. Mombaerts P, Iacomini J, Johnson RS, Herrup K, Tonegawa S, Papaioannou VE. RAG-1-deficient mice have no mature B and T lymphocytes. *Cell*. 1992;68(5):869-877.
16. Schuler V, Lüscher C, Blanchet C, et al. Epilepsy, hyperalgesia, impaired memory, and loss of pre- and postsynaptic GABA(B) responses in mice lacking GABA(B(1)). *Neuron*. 2001;31(1):47-58.
17. Prosser HM, Gill CH, Hirst WD, et al. Epileptogenesis and enhanced prepulse inhibition in GABA(B1)-deficient mice. *Mol Cell Neurosci*. 2001;17(6):1059-1070.
18. Quéva C, Bremner-Danielsen M, Edlund A, et al. Effects of GABA agonists on body temperature regulation in GABA(B(1))-/- mice. *Br J Pharmacol*. 2003;140(2):315-322.
19. Zhu F, Feng M, Sinha R, et al. The GABA receptor GABRR1 is expressed on and functional in hematopoietic stem cells and megakaryocyte progenitors. *Proc Natl Acad Sci USA*. 2019;116(37):18416-18422.
20. Seita J, Sahoo D, Rossi DJ, et al. Gene Expression Commons: an open platform for absolute gene expression profiling. *PLoS One*. 2012;7(7):e40321.
21. Gazit R, Garrison BS, Rao TN, et al; Immunological Genome Project Consortium. Transcriptome analysis identifies regulators of hematopoietic stem and progenitor cells. *Stem Cell Reports*. 2013;1(3):266-280.
22. Nestorowa S, Hamey FK, Pijuan Sala B, et al. A single-cell resolution map of mouse hematopoietic stem and progenitor cell differentiation. *Blood*. 2016;128(8):e20-e31.
23. Olsson A, Venkatasubramanian M, Chaudhri VK, et al. Single-cell analysis of mixed-lineage states leading to a binary cell fate choice [published correction appears in *Nature*. 2019;569(7755):E3]. *Nature*. 2016;537(7622): 698-702.
24. Weinreb C, Wolock S, Klein AM. SPRING: a kinetic interface for visualizing high dimensional single-cell expression data. *Bioinformatics*. 2018;34(7):1246-1248.
25. Erlander MG, Tillakaratne NJ, Feldblum S, Patel N, Tobin AJ. Two genes encode distinct glutamate decarboxylases. *Neuron*. 1991;7(1): 91-100.
26. Baryawno N, Przybylski D, Kowalczyk MS, et al. A cellular taxonomy of the bone marrow stroma in homeostasis and leukemia. *Cell*. 2019;177(7):1915-1932.e16.
27. Choi J, Baldwin TM, Wong M, et al. Haemopedia RNA-seq: a database of gene expression during haematopoiesis in mice and humans. *Nucleic Acids Res*. 2019;47(D1): D780-D785.
28. de Graaf CA, Choi J, Baldwin TM, et al. Haemopedia: an expression atlas of murine hematopoietic cells. *Stem Cell Reports*. 2016; 7(3):571-582.
29. Gessel MM, Norris JL, Caprioli RM. MALDI imaging mass spectrometry: spatial molecular analysis to enable a new age of discovery. *J Proteomics*. 2014;107:71-82.
30. Hardy RR, Carmack CE, Shinton SA, Kemp JD, Hayakawa K. Resolution and characterization of pro-B and pre-pro-B cell stages in normal mouse bone marrow. *J Exp Med*. 1991;173(5): 1213-1225.
31. Petkau G, Turner M. Signalling circuits that direct early B-cell development. *Biochem J*. 2019;476(5):769-778.
32. Chen Y, Yao C, Teng Y, et al. Phorbol ester induced ex vivo expansion of rigorously-defined phenotypic but not functional human cord blood hematopoietic stem cells: a cautionary tale demonstrating that phenotype does not always recapitulate stem cell function. *Leukemia*. 2019;33(12):2962-2966.
33. Capitano M, Zhao L, Cooper S, et al. Phosphatidylinositol transfer proteins regulate megakaryocyte TGF-β1 secretion and hematopoiesis in mice. *Blood*. 2018;132(10): 1027-1038.
34. Capitano ML, Mor-Vaknin N, Saha AK, et al. Secreted nuclear protein DEK regulates hematopoiesis through CXCR2 signaling. *J Clin Invest*. 2019;129(6):2555-2570.
35. Mantel CR, O'Leary HA, Chitteti BR, et al. Enhancing hematopoietic stem cell

transplantation efficacy by mitigating oxygen shock. *Cell*. 2015;161(7):1553-1565.

36. Broxmeyer HE, Hoggatt J, O'Leary HA, et al. Dipeptidylpeptidase 4 negatively regulates colony-stimulating factor activity and stress hematopoiesis. *Nat Med*. 2012;18(12): 1786-1796.

37. Gotoh A, Takahira H, Mantel C, Litz-Jackson S, Boswell HS, Broxmeyer HE. Steel factor induces serine phosphorylation of Stat3 in human growth factor-dependent myeloid cell lines. *Blood*. 1996;88(1):138-145.

38. Subramanian A, Tamayo P, Mootha VK, et al. Gene set enrichment analysis: a knowledge-based approach for interpreting genome-wide expression profiles. *Proc Natl Acad Sci USA*. 2005;102(43):15545-15550.

39. Pietras EM, Lakshminarasimhan R, Techner J-M, et al. Re-entry into quiescence protects hematopoietic stem cells from the killing effect of chronic exposure to type I interferons. *J Exp Med*. 2014;211(2):245-262.

40. Holmes R, Zúñiga-Pflücker JC. The OP9-DL1 system: generation of T-lymphocytes from embryonic or hematopoietic stem cells in vitro. *Cold Spring Harb Protoc*. 2009; 2009(2):pdb.prot5156.

41. Krämer A, Green J, Pollard J Jr., Tugendreich S. Causal analysis approaches in Ingenuity Pathway Analysis. *Bioinformatics*. 2014;30(4): 523-530.

42. Miyai T, Takano J, Endo TA, et al. Three-step transcriptional priming that drives the commitment of multipotent progenitors toward B cells. *Genes Dev*. 2018;32(2):112-126.

43. Bowery NG, Hill DR, Hudson AL, et al. (-) Baclofen decreases neurotransmitter release in the mammalian CNS by an action at a novel GABA receptor. *Nature*. 1980;283(5742): 92-94.

44. Kerr DI, Ong J, Johnston GA, Abbenante J, Prager RH. 2-Hydroxy-saclofen: an improved antagonist at central and peripheral GABAB receptors. *Neurosci Lett*. 1988;92(1):92-96.

45. Wardemann H, Yurasov S, Schaefer A, Young JW, Meffre E, Nussenzweig MC. Predominant autoantibody production by early human B cell precursors. *Science*. 2003; 301(5638):1374-1377.

46. Shim J, Mukherjee T, Mondal BC, et al. Olfactory control of blood progenitor maintenance. *Cell*. 2013;155(5):1141-1153.

47. Vega-López A, Pagadala NS, López-Tapia BP, et al. Is related the hematopoietic stem cells differentiation in the Nile tilapia with GABA exposure? *Fish Shellfish Immunol*. 2019;93: 801-814.

48. Astle WJ, Elding H, Jiang T, et al. The allelic landscape of human blood cell trait variation and links to common complex disease. *Cell*. 2016;167(5):1415-1429.e19.

49. Ulirsch JC, Lareau CA, Bao EL, et al. Interrogation of human hematopoiesis at single-cell and single-variant resolution. *Nat Genet*. 2019;51(4):683-693.